Bulk and surface charge states of K3C60

Schiessling, J; Kjeldgaard, L; Kaambre, T; Marenne, [No Value]; O'Shea, JN; Schnadt, J; Glover, CJ; Nagasono, M; Nordlund, D; Garnier, MG

Published in:
Physical Review. B: Condensed Matter and Materials Physics

DOI:
10.1103/PhysRevB.71.165420

Publication date:
2005

Bulk and surface charge states of K_3C_{60}

J. Schiessling,[1,*] L. Kjeldgaard,[1,†] T. Käämbre,[1,‡] I. Marenne,[2] J. N. O'Shea,[1,§] J. Schnadt,[1,‖] C. J. Glover,[3,¶] M. Nagasono,[3,**] D. Nordlund,[3] M. G. Garnier,[3,††] L. Qian,[1] J.-E. Rubensson,[1] P. Rudolf,[2,4] N. Mårtensson,[1,3] J. Nordgren,[1] and P. A. Brühwiler[1,5,‡‡]

[1]*Department of Physics, Uppsala University, Box 530, SE-751 21 Uppsala, Sweden*

[2]*LISE, Facultès Universitaires Notre Dame de la Paix, Rue de Bruxelles 61, B-5000 Namur, Belgium*

[3]*MAX-lab, University of Lund, Box 118, SE-221 00 Lund, Sweden*

[4]*Materials Science Centre, University of Groningen, Nijenborgh 4, NL-9747 AG Groningen, The Netherlands*

[5]*EMPA, Lerchenfeldstrasse 5, CH-9014 St. Gallen, Switzerland*

(Received 3 July 2004; revised manuscript received 11 November 2004; published 18 April 2005)

We detect a significant angle-dependence in the core level and valence line shapes of photoelectron spectra of single crystal K_3C_{60}. This allows the identification of bulk and surface components in the data, and allows us to explain the anomalous line shapes observed for this system. The states near the Fermi level are associated with the bulk of the sample. There is strong evidence of an insulating surface layer, which we ascribe to intermolecular electron correlations. These results simplify the interpretation of previous, apparently conflicting observations.

DOI: 10.1103/PhysRevB.71.165420 PACS number(s): 79.60.Bm, 71.20.Tx, 71.27.+a

I. INTRODUCTION

C_{60} ions in condensed form have an important role in the understanding of high-temperature superconductivity. C_{60}-based salts with alkali metals (A) with stoichiometry A_3C_{60} are well-known to superconduct at temperatures up to 42 K, exceeded only by the copper oxide-based materials.[1] The stoichiometrically neighboring compounds A_4C_{60} are insulating, which is explained by the effects of electronic correlations, lattice symmetry, and vibronic coupling for these narrow-band systems.[2–6] These are so-called "acceptor" compounds, in which each C_{60} molecule is negatively charged as a result of virtually complete transfer of the alkali valence electrons.

A. Previous photoelectron spectroscopy studies of K_3C_{60}

K_3C_{60} has become a primary testing ground for investigations of fulleride electronic structure, presumably because of the ease with which crystals could be prepared. Soon after the first studies[7–9] establishing the existence of stable, composition-dependent phases and a metallic conduction band density-of-states (DOS) at an alkali stoichiometry of 3, however, questions regularly emerged over the complex line shapes measured using photoelectron spectroscopy (PES) for the metallic composition. It was immediately apparent that the narrow bands predicted theoretically[10] were not reflected in the spectra, which were quite broad. This conflict extended as well to the DOS at E_F, which was lower than found using other techniques, and in disagreement with the consensus models of superconductivity in the fullerides.[1] The large size of C_{60} and typical mean free path effects of electrons in condensed materials suggested right away that the presence of a surface compound could be at the root of this conflict.[11,12] Proposals there based on analysis of time-dependent doping of a pure C_{60} film included the idea that the t_{1u} band reflected mainly bulk properties, and that the h_u and deeper bands were strongly affected by the emission from an insulating surface compound. Support for this was also found in the work functions of the samples, as compared to K_6C_{60}; the latter must have a complement of 3 K atoms per fulleride on the vacuum side of the surface fulleride layer, and has a lower work function than K_3C_{60}, consistent with a higher concentration of K on the surface.[12] At the same time, of the two phases, only K_6C_{60} was found to be sensitive to impurities over times of the order of many hours, suggesting that K_3C_{60} had no K layers exposed at the surface.[12] These experiments were performed on mixed-phase samples, however, and yielded at times complex, weak structures which were not duplicated by later workers.

The arguments in favor of a surface phase were countered by the lack of observation of a difference between bulk and surface electronic structure, as measured by varying the emission angle, and thus the degree of scattering of the electrons from subsurface layers,[13] although the existence of such angle dependencies had been asserted in the earlier work.[12] A second observation apparently favoring the similarity of bulk and surface compositions was the lack of strong photon energy dependence reported.[14] Since it was, moreover, possible to describe the broad conduction band line shape in terms of coupling to vibrations and plasmons,[13] a broad consensus along the lines of bulk-surface equivalence developed, with electron-electron correlations and electron-plasmon coupling implicated for the complex spectra observed.

After this initial group of publications, a method of quite reliably producing purified single-composition samples *in vacuo* for PES studies was reported.[15] It was applied to new studies of the PES of K_3C_{60} first several years later.[16] There it was found that the line shape reported earlier[13,17] for the lowest unoccupied molecular orbital (LUMO)-derived conduction band was largely reproduced, albeit sharper for the more highly purified samples. No major angle dependence of the conduction band spectrum could be detected, supporting the earlier consensus view.[13,16] Later, similar arguments and a similar lack of visible surface effects in electron energy

loss spectra (EELS) of the same samples further strengthened this viewpoint.[18]

B. Open questions on the PES of K_3C_{60}

While the lack of an observed difference between surface and subsurface (bulk) layers of K_3C_{60} can perhaps suffice to maintain that deduction as the consensus,[13,14,16,18] there are a number of observations which are nontrivial to reconcile with this view, aside from those already discussed.[11,12] We will list these in what follows as a critical review of the current state of the field of PES studies on the superconductor fulleride phases, which is necessary to understand how the present results unify a number of apparently conflicting interprations of K_3C_{60} PES spectra. Readers not needing a detailed review may wish to skip to Sec. I C.

1. Temperature dependence

A strong temperature dependence in the data was detected quite early,[13] which amounted to a washing-out of the DOS at E_F at room temperature. No clear explanation for this was offered, but the correlation of the DOS at E_F with the first portion of the highest occupied molecular orbital (HOMO)-derived band in this respect was noted.[13] This observation was later duplicated and attributed to strong electron-electron correlations splitting the conduction band further than previously speculated, i.e., to a degree involving partial overlap with the HOMO-derived band.[19] Given the different models of the valence spectra offered,[13,19] the reason for the similar temperature-dependence of the strong portion of the LUMO-derived band with the weak portion of the HOMO-derived band remains an open question.

2. Charge-charge correlations and spectral widths

Possible roles of charge-charge correlations in the spectra have been discussed[13,14,17] since the first spectral consequences were reported.[14,20] The likelihood that they could be an important source of broadening, as opposed to vibrations and plasmons,[13] has been implicated after the repeated observation of simpler (and narrower) spectra of K_3C_{60} monolayers adsorbed on silver substrates,[21,22] thus supporting early arguments.[20] This difference was thought to be connected to the added presence for a monolayer of substrate-derived image screening,[23] which reduces the intramolecular charge-charge correlation energy U by about half. It is not clear, however, why a reduction of the scale of correlations by a factor of about 2 should almost totally quench their broadening effects, which is implied by the fact that the spectra of the Ag-adsorbed monolayers strongly resemble those of pure C_{60} and K_6C_{60} in width.[14,21] In a model of dominant intramolecular correlations, one would expect a shift of spectral weight by the change in U,[24,25] i.e., from about 1 eV from the main line to about $1/2$ eV, which is not observed, as we reconsider in Sec. III E. In addition, the HOMO-derived band for doped monolayers has a sharp low-binding-energy onset,[16,21] reminiscent of that of K_3C_{60}, in keeping with the correlation of E_F and this shoulder already noted above and in previous work.[13,19] Perhaps the most important challenge to the idea of correlation satellites is, however, that they are not reflected similarly in the spectra of different bands; for the LUMO-derived band the low-binding-energy structure, or main line, is strongest, whereas in the remaining portion of the valence spectra and the C 1*s* line the intensity of the higher-binding-energy structures, or ostensible satellites, is much greater than the main line, contrary to general expectations in such a picture.

3. K distribution at the surface

The C 1*s* line of K_3C_{60} is one of the broadest measurable for an intact molecule.[14,19,26] Since chemical shifts are well-known to affect core level binding energies,[24] a natural explanation for such broadening is a distribution of C-atom sites. Such a distribution is established in the bulk of K_3C_{60} due to the Madelung potential exerted by the alkali ions, as well as the molecular charge distribution, which splits the degeneracy of the carbon atoms into three distinguishable sites with a ratio of 2:2:1. This was therefore adopted as an explanation of the splitting observed for the highly pure sample.[26] Theoretically, however, the local charges differ only slightly, and the effects due to this are expected to be small.[27] This would also require that 1.5 surface K ions per fulleride molecule adopt positions and exert fields consistent with the bulk structure, although the lack of further fulleride neighbors could be expected *a priori* to induce them to approach the surface molecules more closely than in the bulk, and to exert stronger fields. This merely points out that the conditions for exactly a 2:2:1 ratio of C-atom sites are not trivially fulfilled at the surface with the given assumptions, whereas violations of the assumptions would not be surprising.

Further evidence that such a bulklike model must be reexamined comes from monolayer studies. Examining the C 1*s* line in such cases,[28–32] one generally finds much narrower lines, without an obvious, large substructure as for K_3C_{60}.[14,19,26] In addition, no strongly-split, broad line has been reported for a K_3C_{60} monolayer supported on a metal substrate. These facts in themselves suggest that drastically different local chemical environments for different C atoms on a given molecule are not sufficient to explain such large chemical shifts in the bulk fulleride. On the other hand, the general lack of such shifts in verifiably asymmetric potentials can be rationalized[31] as being due to the excellent intramolecular screening afforded by the fullerene,[33,34] which apparently is sufficient to reduce such potential differences to small levels on the scale of the linewidth. The large width and obvious splitting[26] of the C 1*s* line of K_3C_{60} must therefore be considered an open question, more a challenge to the consensus model than a support.

4. Macroscopic electric fields and the possibility of a half-valence compound in the surface layer

Quite recently in the history of the field, it was pointed out that there are fundamental reasons to assume from first principles that the surface composition of K_3C_{60} could be quite different from the bulk.[35] The layers of fullerene and potassium can be considered to be stacked in the (111) direction, which is also the direction exposed at single crystal

surfaces studied so far.[16,17,35,36] This stacking leads to strong local fields, as is well known, they being the basis of the Madelung potential. At the surface, however, it is important to compensate these fields, since otherwise, just as at the surface of a capacitor, macroscopically (and nanoscopically) huge fields would arise, which is not observed. This allows a few possible scenarios.[35] One involves the standard bulklike termination, but two lead to termination with fulleride charges of −1.5 or −2.5.[67] The −1.5 charge state entails a structure which exposes no potassium at the surface, therefore offering a natural explanation for why K_3C_{60} is very robust in standard UHV chambers for many hours, whereas K_6C_{60} is relatively reactive.[12,35] We return to the question of the surface composition below, and simply note that the electrostatic considerations brought forward there represent a significant challenge to the consensus model in their own right. Since the sample preparation approach of Ref. 35 was somewhat different than the recommended recipe,[15,16] it is perhaps understandable that small differences in the spectra and interpretation of the DOS at E_F arose in that study. It is, however, noteworthy that one observation was used to suggest that the heat-treated samples were underdoped in the surface layer, namely that the DOS at E_F increased if those samples were exposed to fractions of a monolayer of K.[35] This is intriguing because of the simultaneous growth of the low-binding-energy shoulder of the HOMO band, i.e., a correlation similar to that seen in a previous growth study,[17] and in the temperature dependence.[13,19] Indeed, this shoulder and the DOS at E_F are both strongest at the same composition,[17,35] above which another phase, K_4C_{60}, begins to form. Thus the temperature and doping dependencies require that a successful model of the system explain the excellent correlation of the strong portion of the LUMO-derived bands with the weak portion of the HOMO-derived bands.

5. The bulk intensity in the spectrum and the mean free path in K_3C_{60} photoemission studies

We now want to address the question of the surface sensitivity of the PES spectra, which has thus far been characterized in terms of the electron mean free path. This is necessary due to the emphasis placed upon this point by recent proponents of the dominant concensus[16,19,26] as well as opposing[25,35,37] viewpoints, claiming that only the surface electronic structure is observed in the spectra. We present here, therefore, a rather in-depth examination of the previous work on this issue. The simplest way to discuss the surface sensitivity is under the assumption that a photoelectron travels from the point of origin along a straight line trajectory, with a certain probability of inelastic scattering on the way to the sample surface. The ensuing attenuation of the photoemission signal can be described by a simple exponential law, under which the average distance that photoelectrons travel along the trajectory between inelastic collisions is given by the inelastic mean free path (IMFP).[39]

Concerning the surface sensitivity of C_{60} systems, the reference cited most is the study by Wertheim *et al.*[11] That work compares $C_{60}/Cu(111)$ overlayer experiments and previous results of C_{60} and K_3C_{60} multilayers with the calculated IMFP for amorphous carbon.[40] Some of the experimental IMFP values were shifted downwards by about 50% to match the theoretical curve. This was explained as a correction due to an assumed nonlayerwise growth of the C_{60} film on Cu(111). The corrections applied to the overlayer data were applied as a conservative estimate of the maximum possible effect of scattering, i.e., to explore the reasonable lower limit on the bulk contribution. However, there is reason to question some of the assumptions of Wertheim *et al.* For instance, the curve by Tanuma *et al.*[40] used there is calculated for single crystal and amorphous elements. In a follow-up paper, Tanuma *et al.* show that the IMFP of organic compounds is generally larger than those of elements.[41] Details on the calculation of the IMFP are given in the Appendix. There we see as well that, primarily because of its lower density, C_{60} is expected to have one of the highest IMFP for condensed materials, ignoring possible structural effects such as diffraction. For the analysis in the present study photoelectrons with a kinetic energy of about 100 eV are considered rather important. For this energy Wertheim *et al.* report an IMFP of 6 Å.

Goldoni *et al.* evaluated the IMFP from PES and EELS measurements. Their values of the IMFP are displayed together with a fitted curve.[18] This fit gives lower values than expected from the theoretical work of Tanuma *et al.* for amorphous carbon and for organic compounds.[41] Their PES data are taken from an overlayer study of $C_{60}/Ag(100)$ and the coverage is estimated by the ratio of the C 1*s* to Ag 3*d* photoemission signal. They also employ EELS data taken for a wider range of excitation energies by comparing the attenuation of the intensity of the interface layer with that of the surface layer for a bilayer of $C_{60}/Au(110)$. Unfortunately, there are no structures in the interface layer EELS data in the energy interval used, which makes such intensity estimates nontrivial. The value of the IMFP at kinetic energies of 100 eV is reported to be 5 Å.

Maxwell *et al.*[28] show the development of the C 1*s* photoemission line shape for increasing numbers of layers C_{60} on Au(110). The C 1*s* line of the bilayer can be decomposed into contributions from surface (62%) and interface (38%) layers. Assuming a simple exponential decay of the photoemission signal, the ratio of the contributions yields an IMFP of 16.3^{+25}_{-8} Å for 100 eV kinetic energy electrons.[42]

Given the large difference between the third and previous two values, it seems necessary to consider the sensitivity of the IMFP to the determination of the bulk contribution to the spectrum. As we show in detail in the Appendix, the apparent disagreement among the results reported is due to an emphasis on expressing them in terms of the IMFP. In terms of intensity, on the other hand, the contribution from bulk molecules to PES of C_{60} solids agrees within the uncertainties for all three studies and can be expected to be in the range of 20%–30% of the total photoemission signal for kinetic energies near 100 eV. This puts additional constraints on any model of the electronic structure near the surface.

C. Summary of previous work and outline of present paper

To summarize, the broadest consensus seems to be that the signal from subsurface layers is not represented in PES

spectra, and a majority of researchers in the field have apparently assumed that bulk and surface of single-crystal K_3C_{60} have the same composition. Furthermore, at least one plausible model for the LUMO line shape has been proposed[13] in terms of a K_3C_{60} surface stoichiometry, but no plausible explanation of the deeper levels, including the C 1*s*, has emerged. The idea that intramolecular correlation effects somehow lie at the root of the complex line shapes observed in PES has not been borne out by any study this far. Thus the claim that the surface signal dominates to the extent that a subsurface (bulk) signal is impossible to measure,[18,19,35,37] in contrast to an early point of view,[12] is valid only to the extent that a 20%–30% signal cannot be extracted.

We show that the substructure in the C 1*s* and deeper valence levels have the same origin, which we attribute to different K concentrations in surface and bulk. This similarity between different spectral regions is explained by an almost universal tendency of the deeper valence and C 1*s* levels to shift uniformly as a function of K doping level (for crystalline phases) or charge transfer in general, a tendency overlooked by previous workers. The bulk is found to be metallic, and the surface to be a largely insulating compound (perhaps weakly metallic) from the spectra alone. Assuming a surface charge of −1.5 per fulleride consistent with the field-neutralization[35] and chemical inertness requirements,[12,35] we are able to explain these observations in terms of the allowed charge states at the surface and the known intermolecular correlation energy, V,[43] as well as the intramolecular term, U. The surface compound emerges naturally in this picture, and is explained in terms of a correlated insulator, with a gap (or pseudogap) given by $2V$.

II. EXPERIMENTAL DETAILS

The experiments were carried out at Beamline I511 at MAX-lab.[44] A standard UHV preparation chamber with a base pressure of 2×10^{-10} mbar was employed. A film 300 Å thick was prepared layer-by-layer in increments of approximately 30 Å *in situ* on a Cu(111) substrate, alternating C_{60} and K deposition. C_{60} was evaporated from a homebuilt crucible, and K from an SAES getter source which was activated in the UHV chamber. After each deposition cycle the stoichiometry was checked with PES, using published spectra[15,19] as references. After the deposition was completed the sample was annealed at 600 K for 6 h to sublime excess C_{60}, resulting in a single phase.[15] The sample spectra at 100 K compared well with previous studies.[19,26,35] A (1×1) (111) low-energy-electron-diffraction (LEED) pattern was observed, consistent with previous work on K_3C_{60} crystal surfaces.[16,17]

The spectra were taken using linearly polarized undulator light incident at about 82° from normal; note that the direction of radiation incidence was (almost) in the plane of the sample surface. The sample holder was supported in a chamber which could rotate around this axis due to special pumping and support constructions. Hence both sample and analyzer could be rotated independently around the light incidence axis in order to change the detection direction relative to the light polarization and sample normal. We found that aligning the spectrometer to the polarization direction minimized the effects of scattered photoelectrons as observed[42] for solid C_{60}, which we discuss in more detail in Sec. IV. However, the same general trends in the photoemission spectra are observed if the polarization is fixed along the sample normal. Grazing emission will be used to refer to collection of the electrons at 70° from normal. The photon energy was 402 eV for the C 1*s* and K 2*p* spectra, and 110 eV for the K 3*p*, valence, and LUMO-derived spectra, with total energy resolutions (analyzer acceptance angles) of 150 meV (±9°) for C 1*s* and K 2*p*, 80 meV (±6°) for valence, and 40 meV (±4°) for LUMO-derived spectra. Combined with the kinetic energy of just over 100 eV, this implies that electrons are collected from the entire Brillouin zone. All spectra were corrected for the nonlinear transmission function of the photoelectron analyzer.[45]

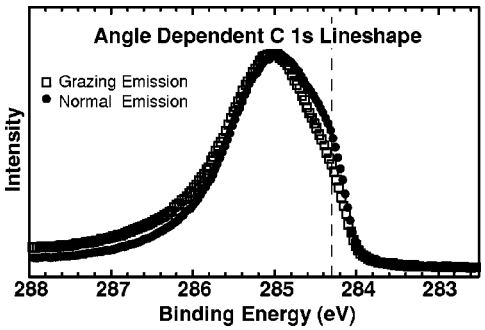

FIG. 1. C 1*s* photoemission spectra of K_3C_{60}, measured at the indicated angles.

III. RESULTS AND DISCUSSION

A. C 1*s* PES

We begin the presentation of our data with the C 1*s* spectra, which are simpler to analyze than the valence data. C 1*s* PES is shown in Fig. 1. There is an obvious angle dependence in the shoulder at 284.3 eV. This observation suggests that the C 1*s* line consists of at least two components. The weaker one is located primarily at low binding energy and the stronger one at high binding energy. The component which becomes weaker at grazing emission is assigned to subsurface molecules, leaving the dominant component as a surface contribution. One observes intensity variations of at most about 20% in x-ray photoelectron diffraction on C_{60} monolayers,[46] and since such intensity variations have not been observed in valence PES for solid C_{60} samples,[42] we rule out an important role for diffraction in our observation. The angle dependence suggests, moreover, that the intensity ratio depends on the choice of emission angle, and rules out the previous analysis in terms of chemical shifts due to different carbon sites.[26]

We would therefore like to avoid strong assumptions regarding the line shapes. The large binding energy shift deduced for the components in Fig. 1 suggests that not all molecules have the same charge, according to the discussion in Sec. I B 3, i.e., that some may not be in a metallic state. Hence the proper choice of line shapes for a reasonable *a*

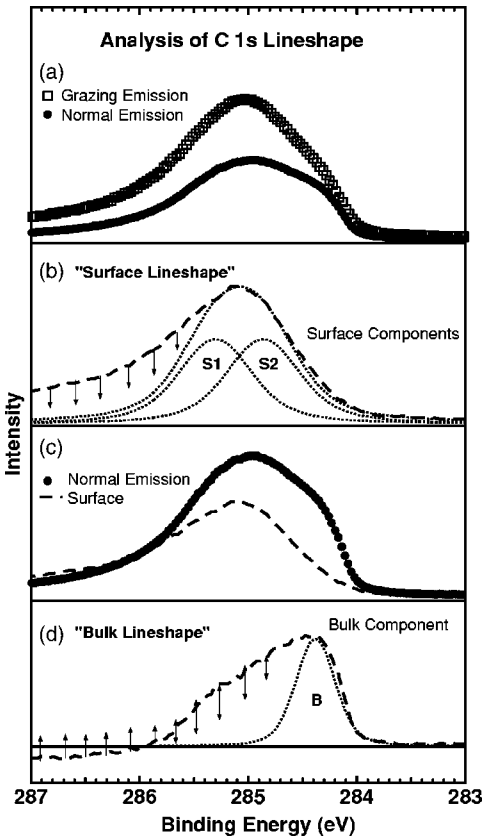

FIG. 2. (a) C 1*s* photoemission spectra of K_3C_{60} at the indicated emission angles, scaled to give similar intensities for the shoulder at 284.2 eV. (b) The dashed line is the difference spectrum between normal and grazing emission as scaled in (a). The other curves are discussed in the text. (c) Normal emission spectrum and surface line shape, scaled to extract the bulk component. (d) Approximate bulk line shape obtained as the difference derived from the spectra in (c). The dashed line illustrates a plausible main line for a metallic line shape. Also shown are suggested corrections (arrows) due to the influence of scattered electrons. See the text for more details.

priori decomposition of the spectrum becomes difficult. We chose an empirical approach instead. To determine an approximate empirical line shape for the surface component, the two spectra of Fig. 1 were scaled to match at the shoulder. One measure of the scaling factor is the shape of the tail in the low binding energy region in the difference spectrum, which should be similar in shape to the grazing emission spectrum. Taking this into account it is possible to scale the normal and grazing emission spectra to have similar bulk contributions, as illustrated in Fig. 2(a). The difference spectrum gives an empirical profile for the high-binding-energy component, as displayed in Fig. 2(b). The high-energy tail is likely to be too strong due to the effects of scattered photoelectrons for grazing emission, and can probably be corrected in the manner suggested by the arrows. The dotted lines show two Gaussians and their sum. The meaning of the curves S1 and S2 will be taken up later. The resulting line shape strongly resembles the grazing emission spectrum. It can now be employed to obtain an estimate of the bulk spectral profile via a similar subtraction procedure using matching at high binding energy, as illustrated in Fig. 2(c), with the result shown in Fig. 2(d) representing the empirical bulk line shape. We surmise that this difference spectrum should be corrected as suggested by the arrows, due to the overly large scattered electron intensity at high binding energies in the spectrum of Fig. 2(b). The shape of the difference spectra turns out to be rather robust, which means that even for slightly different relative scaling of the original curves the empirical line shape does not change much, in particular the empirical bulk line shape is always asymmetric with a tail towards higher binding energies. Nevertheless, the two components give an impression of where the main intensity from the bulk and surface contributions are found in the spectra, and of their profiles.[68] Linear combinations of the two components, scaled to match the total at each angle, are shown as solid lines in Fig. 3(a) and 3(b). This enables us to estimate the amount of bulk contribution in the spectra, giving $(29\pm10)\%$ in normal and $(17\pm10)\%$ in grazing emission. This compares well with previous work, as discussed in Sec. I B 5, and the metallic character is consistent with bulk transport measurements.[1]

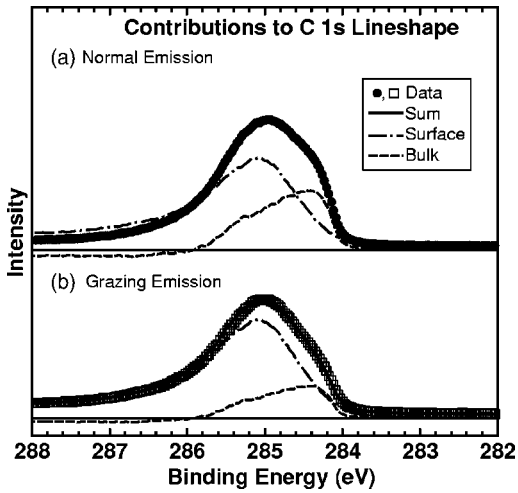

FIG. 3. C 1*s* photoemission spectra at the indicated emission geometries, with the relevant surface and bulk contributions obtained from the line-shape analysis shown in Fig. 2. Both components are recombined to fit the normal and grazing emission data, with the result shown as a solid line. See the text for a discussion.

B. Valence bands

The photoemission spectrum of pure C_{60} shows a clear separation between the highest occupied molecular orbital (HOMO) and the next band (HOMO-1). In contrast, the valence line shape of K_3C_{60} consists of broad structures, hampering a straightforward spectroscopical identification of individual MOs. This width has been discussed in the literature in terms of plasmon excitation[13] and correlation satellites.[25] A plasmon excitation at 0.6 eV has been measured by different techniques,[18,47] motivating its use in models of the spectra, but not ruling out possible correlation satellites.

Most studies of the K_3C_{60} valence band focused on the LUMO-derived line shape. Before discussing this, we want to analyze structures in the fully occupied valence region. A typical valence spectrum is shown in Fig. 4. Similar to that

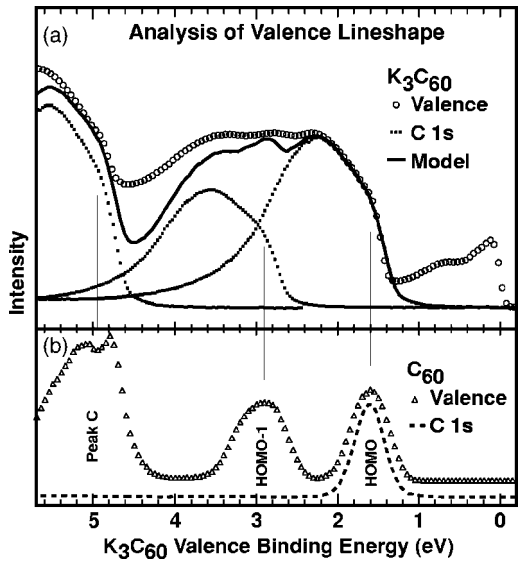

FIG. 4. (a) Normal emission valence PES spectrum of K_3C_{60}. The solid line is a model given by the sum of the illustrated images of the normal emission C 1*s* spectrum (dashed lines), placed according to the peaks of pure C_{60} as suggested by the vertical lines. (b) Comparison with a pure C_{60} spectrum (shifted in energy) to help illustrate the uniform shifts. See the text for more details.

of the C 1*s*, the valence line shapes are broad, with a shoulder or weak structure at the onset of *each* filled band (e.g., at 1.6, 2.9, and ~5 ev). We observe an excellent correspondence between the HOMO-derived and C 1*s* spectra, seen in the matching at the onset of the HOMO-derived band. This correspondence is found to be valid also for the other filled levels to first order, since the K_3C_{60} valence spectrum can be modeled by summing replicas of the C 1*s* separated according to the levels of pure C_{60}, as indicated. We see that all the subtle features in the K_3C_{60} spectrum are reproduced semiquantitatively by this method. Not only does this suggest a preserved one-to-one correlation between the electronic structure of C_{60} and K_3C_{60} as indicated in the figure, but also that the width of the K_3C_{60} features is due to the same mechanism(s) which determine the C 1*s* line shape.

This coincidence in valence and core level shifts has been noted previously[31] for C_{60}, but has not been discussed more generally, and in particular not for fullerides. That the levels in C_{60} systems show a constant energy separation upon charge transfer is summarized in Table I. We have included all data from charge transfer systems which we could locate in the literature, selected using the following criteria: (a) We require C 1*s* and valence photoelectron spectra calibrated in energy with respect to each other, so only references containing both data may be included; and (b) we need cases for which the bonding is expected to have predominantly charge transfer character, to be able to neglect hybridization-induced shifts. Shifts and other distortions due to covalent bonding are reported, e.g., for certain levels of C_{60}/Au,[28] C_{60}/Al,[31] C_{60}/Ni,[32] C_{60}/Pt,[32] C_{60}/Si,[50] and C_{60}/InP.[51] Since we focus here on the HOMO, cases in which the HOMO appears unaffected by such interactions, such as C_{60}/Au(110), are included. Table I shows clearly that the shifts are, to within 0.1 eV, constant for all ordered systems in which charge

TABLE I. C 1*s* and HOMO-derived binding energies for the indicated samples, illustrating the uniform shifts of these levels in cases of charge transfer bonding.

Reference	Sample	C 1*s* (eV)	HOMO -derived (eV)	ΔE (eV)
Maxwell *et al.*[48]	Solid C_{60}[a]	289.6	6.9	282.7
Goldoni *et al.*[19]	K_4C_{60}	285.0	2.3	282.7
Brühwiler *et al.*[14]	K_6C_{60}	285.1[b]	2.3	282.8
Goldoni *et al.*[19]	K_3C_{60}	285.0	2.3	282.7
Present work	K_3C_{60}	285.0	2.3	282.7
Maxwell *et al.*[28]	C_{60}/Au(110)	284.4	1.7	282.7
Tzeng *et al.*[49]	C_{60}/Au(111)	284.5	1.8	282.7
Tsuei *et al.*[30]	C_{60}/Cu(111)	284.2	1.6	282.6
Magnano *et al.*[29]	C_{60}/Ag(110)	284.4	1.8	282.6
Pedio *et al.*[32]	C_{60}/Ag(111)	284.5	1.9	282.6

[a]Ionization potential, referred to vacuum level.
[b]Unpublished.

transfer to the LUMO is involved, within the given criteria. This pattern has also been reported for the valence and core levels of K-doped graphite[52] and carbon onions.[53] As previously discussed,[31] we attribute this to the efficient internal screening[33,34] of a core hole in C_{60}, which makes the final state charge distribution similar to that of a valence hole, and thus the external screening contributions quite similar. The existence of identical shifts for the valence and C 1*s* levels confirms that the small variations in charge density found[27] for different carbon sites in K_3C_{60} cannot be the cause of the splitting in the C 1*s* line,[26] consistent with the discussion in Sec. I B 3 and in the results of Sec. III A.

As noted in Sec. I B 4 there is a clear trend that, upon deposition of K onto C_{60}, the shoulder below the HOMO-derived band and the intensity at E_F behave similarly, as shown in Fig. 1 of Ref. 17 and elsewhere.[35] At the same time, the main part of the HOMO-derived band and the intensity at the higher binding energy side of E_F also vary in a coordinated manner, suggesting that the LUMO is also to be included in the phenomenon collected here of uniform shifts. Indeed, successive K doping of C_{60}/Si shows a rigid shift of all the valence levels.[54] In Fig. 1 of Ref. 21, the shape of the LUMO-derived band changes, but the energy difference between the "LUMO" and "HOMO" is constant for all K concentrations. Fig. 2 of the same reference shows that the peaks ("LUMO," "HOMO," and "HOMO-1") of ML "K_3C_{60}" coincide with the shoulders and peaks of solid K_3C_{60} which we assign to the metallic bulk phase, similar to C_{60}/Ag(100) in Fig. 3(b) of Ref. 16. Successive intercalation, e.g., in Merkel *et al.*,[55] yields a constant energy difference between the HOMO-derived and C 1*s* bands of 282.7 ± 0.2 eV. Thus all available data on bulk fullerides and a number of other charge transfer fulleride systems are consistent with the present model of a uniform shift of all levels in C_{60} upon charge transfer, as a function of charge state. This rationalizes the excellent correlation between the fully occupied levels and the C 1*s* in Fig. 4(a). Hence the observed uniform

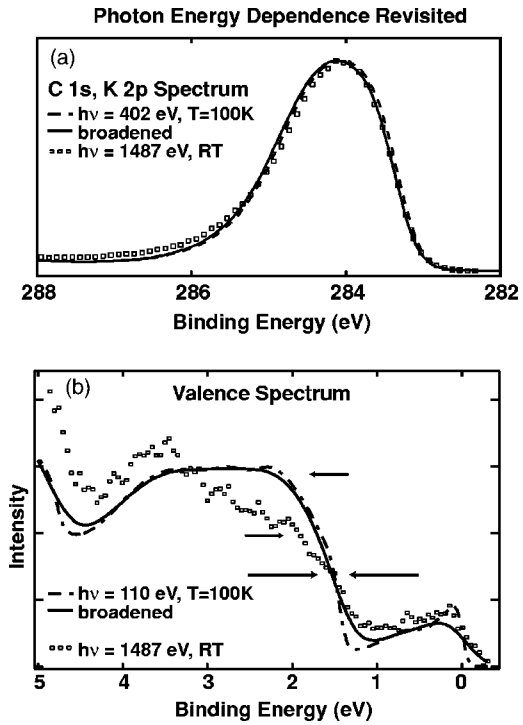

FIG. 5. Valence and core level data of K_3C_{60} taken at the indicated photon energies. The 1487 eV data (Ref. 14) were taken at 45° emission with unpolarized light, the 110 eV data at normal emission and with the light polarization along the emission direction. The 110 eV data are broadened (solid line) to mimic the effects of the poorer instrumental resolution at 1487 eV. (a) Normalized core level spectra. Taking differences in emission angle and IMFP into account both spectra are expected to have similar surface and bulk contribution. (b) The valence PES are scaled to match at the shoulder as indicated by the long arrows. The small arrows indicate the surface peak intensities. See the text for more details.

shift in the present work is further and more conclusive evidence for the existence of different molecular sites near the sample surface, differentiated by their charge state and presence or lack of metallic character, as suggested above based on the C 1*s* spectra.

C. Photon energy dependence

After establishing the existence of distinguishable surface and bulk signals in the spectra via angle-dependent PES, we now want to turn to the photon energy dependence in the spectra to provide a cross-check of our interpretation. We will compare the present carbon and potassium data to spectra excited with Al $K\alpha$ radiation.[14] Due to the higher kinetic energy of the photoelectrons for Al $K\alpha$ excitation, the signal from the bulk is expected to be increased. In Fig. 5 we compare the valence band and core level PES of K_3C_{60} taken at 110 eV (dashed line) with high excitation energy data (circles). A version of the former is shown convoluted with a Gaussian to facilitate the comparison in a first approximation of the effects of the poorer resolution in the x-ray spectra.

For the interpretation of the comparison it is important to recall that the bulk signal in the high energy data is expected to be attenuated for two reasons: (1) the spectrum was taken at 45° emission from the surface normal and (2) the light was not strongly polarized. To estimate the IMFP at 1200 eV kinetic energy, we use the centroid of our own determination of the bulk/surface intensity ratio as the relevant measure of the IMFP at 100 eV, and extrapolate. The intensity is estimated using Eq. (A1) in the Appendix.

The core level data are shown in Fig. 5(a). The spectra have similar line shapes, especially after broadening the low-energy data. The intensity on the low binding energy side is quite similar, suggesting similar bulk contributions. Given the emission angle difference, this is consistent with a larger bulk contribution in the C 1*s* data at higher excitation energy. The broad line shape allows no more detailed analysis.

The high noise level hampers a detailed analysis of the LUMO-derived region in Fig. 5(b); however, the comparison shows that the apparent agreement at different photon energies is due to the small expected differences in the LUMO region, which can in turn be attributed to the relatively weak surface LUMO emission. The HOMO-derived band is difficult to assess, due to the poor statistics. This is a consequence of the much lower valence cross section at x-ray energies, and causes a sloping background in the data as well, as can be appreciated upon comparing the data of Ref. 38 with those in Fig. 4. We attempt to indicate the heights of the shoulder and peak positions (2.2 eV) of the HOMO-derived bands. Starting from the LUMO-derived backgrounds in each spectrum, the peak-to-shoulder ratios are about 2:1 in the low-energy, and perhaps 1.5:1 in the high-energy spectra, respectively. This is consistent with the C 1*s* data, though not quantitatively precise. It is also consistent with expectations of higher bulk intensity, modified by a reduction due to the more grazing emission angle. The bulk-to-surface ratio in both spectra is then expected to be of the same order of magnitude, as observed. The K spectra show a photon energy dependence as well, in line with our model of different surface and bulk sites, which is discussed together with its angular dependence below in Sec. III F.

D. Electrostatics and surface vs bulk structure revisited

As already discussed,[12,16,37] the spectra are derived predominantly from the surface layer, which in addition to the observed angle dependence motivates our assignment above of the weaker, low-binding-energy component of the C 1*s* and valence PES to molecules in the bulk. This assignment implies that the Madelung potential due to screening and/or charge states is significantly different in the surface and bulk layers. Here we want to take up the crystal structure, based on the excellent discussion by Hesper *et al.*,[35] in order to motivate the implications to be drawn from our data. The basic points after considering the electrostatics of the ionic compound K_3C_{60} were described in Sec. I B 4. There are three possible energetically stable surface configurations, with an outermost layer and charge state of either $C_{60}^{-1.5}$, K^{+1}, or $K^{+1.5}$. Our sample and others[12,16,35] are quite stable against contamination over the period of preparation and measurement over tens of hours, which is not the case for K_6C_{60}, leading us to exclude the possibilities that the outermost

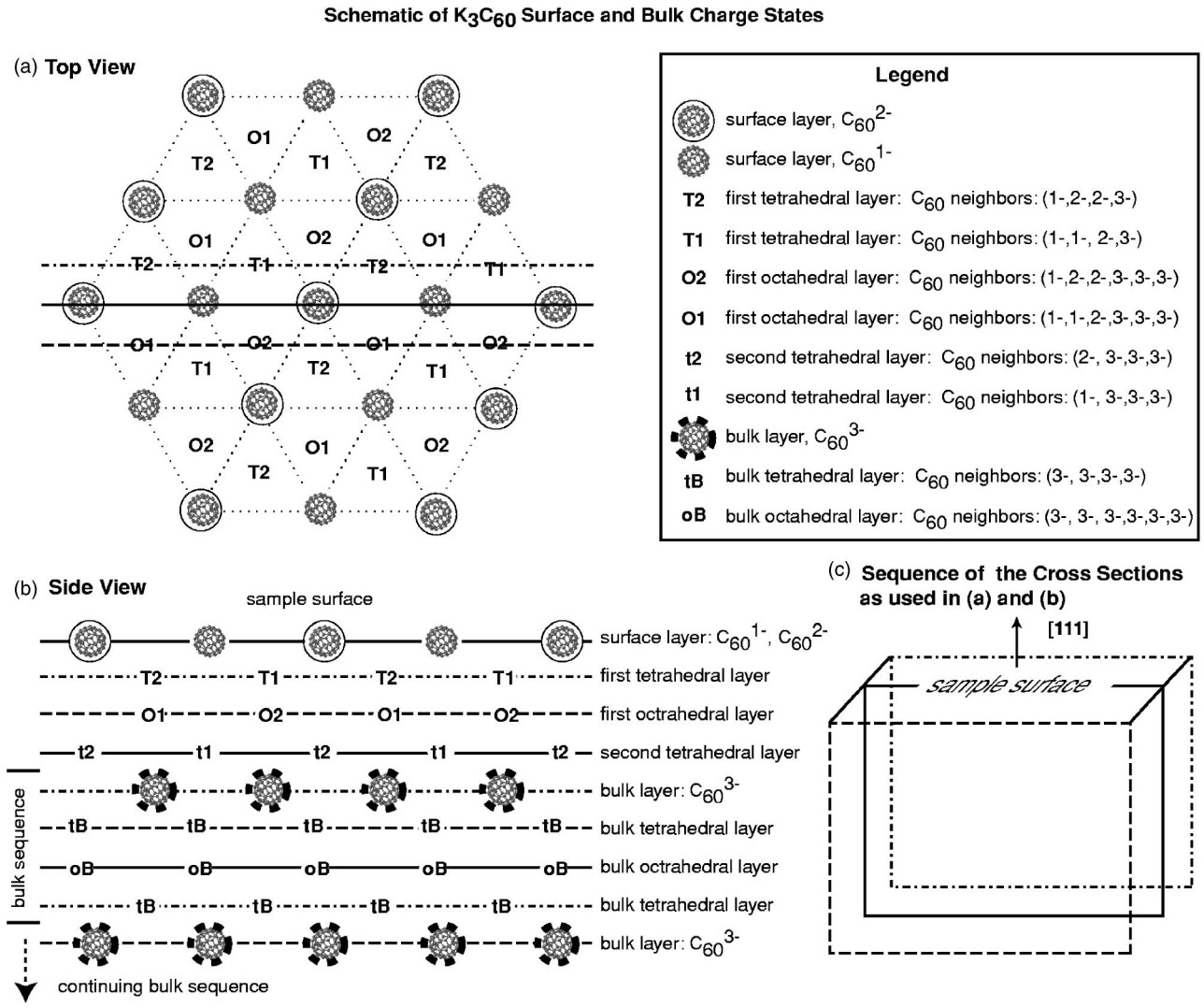

FIG. 6. Schematic of the lattice sites of the K_3C_{60} surface and immediate subsurface regions. Fulleride sites are indicated by molecular images, K ions by letters and/or numbers. The charge states of the molecules are indicated by the absence or presence (and type) of circles around the molecular images, as specified in the legend, along with details of the local charge configurations for particular sites. (a) View from the top of the K_3C_{60} (111) surface, in which only the outermost layer of fulleride ions is visible, seen to consist of C_{60} molecules in charge states −1 and −2. The potassium ions of the three layers below are shown as well. To help illustrate the stacking sequence, three cross sections are taken, indicated by the horizontal lines. (b) Side view of the three cross sections suggested in (a). Height in this figure corresponds to vertical placement, and horizontal placement depicted by the three cross sections is indicated by the dashing of the lines through a given set of sites. This figure allows one to assess the qualitative variation in Madelung potential. (c) 3D illustration of the arrangement of the slices indicated by the horizontal dark lines in (a) and (b).

layer consists of reactive alkali ions. This leaves only the case in which the outermost layer of K_3C_{60} consists of C_{60} planes with an average molecular charge of −1.5. Figure 6(a) depicts the (111) surface layer, with the C_{60} molecules forming a hexagonal lattice as obtained by LEED and STM.[36] As is well-known, the voids between the molecules correspond to the tetrahedral and octahedral lattice sites, located below the surface C_{60} layer, which are occupied by potassium ions. In Fig. 6(b) the particular stacking sequence along the ⟨111⟩ direction is shown. Planes of single C_{60} layers alternating with three planes of K layers form alternating charge planes. The slices to which the planes belong are indicated in Fig. 6(c). This structure will form the basis of discussion in what follows.

E. LUMO PES

Clearly the conduction band, derived from the lowest unoccupied molecular orbital (LUMO) of C_{60}, is generally the most interesting aspect of the electronic structure of a superconducting compound, which explains the multitude of studies aimed at this portion of the electronic structure, often to the exclusion of most of the rest of the bands. This portion of the spectrum is arranged oppositely to all others, with a maximum at low binding energy, and a minimum at higher binding energy, exposing the fundamental difficulty in explaining all portions of the spectrum simultaneously.

Figure 7 shows an expanded view of the LUMO-derived PES collected both in normal and grazing emission. The grazing emission spectrum compares well with previous data

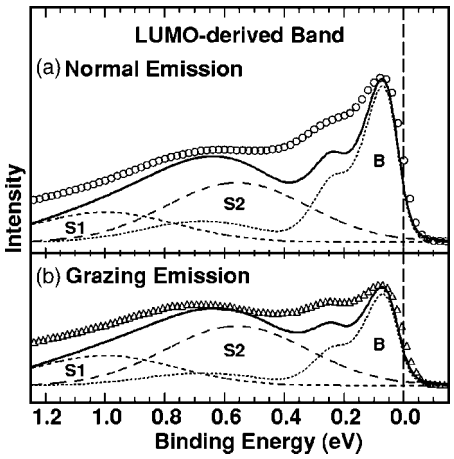

FIG. 7. LUMO-derived band of K_3C_{60} for the indicated emission angles. The light polarization is always parallel to electron emission direction. The model shown is described in the text.

at other angles.[13,16,35] The ratio of the peak height at E_F to the signal at 1.3 eV in the normal emission spectrum is greater than in all previous reports, however. This is due to the experimental geometry and, in particular, the use of polarized light, which we address in more detail in Sec. IV. The angle dependence shows that the intensity at E_F drops with increased emission angle, suggesting that the emission at E_F is associated with the subsurface (bulk) electronic structure. This is consistent with the results for the C 1*s* line. This angle dependence and the uniform shifts expected for all the levels suggest that the near-E_F region of the spectrum has a significant bulk component, but leaves open the question of the characteristics of the surface component, although the lack of intensity at lower binding energy of this component for the C 1*s* and, by implication of the analysis in Sec. III B, HOMO-derived and deeper valence bands, suggests that the surface components derive from an insulating compound. We will now use the results obtained and deduced thus far to assemble model LUMO-derived spectra for both angles in terms of bulk (B) and surface (S1,S2) contributions, as shown.

To construct a model of this spectrum, it is necessary to have a clearer view of which charge states are involved at the surface, for which we refer to Fig. 6(a). A half-integral average surface charge state of −1.5 as inferred in Sec. III D corresponds to half of the molecules at a charge of −1, and the other half at −2, since the molecular nature of the sample requires near-integral local charges.[56] K_3C_{60} is, as reviewed in Sec. I, a correlated material, in which the intramolecular Coulomb repulsion U tends to drive the system toward an insulating state, whereas kinetic energy terms, represented by the one-electron bandwidth W, aided by Jahn-Teller coupling, tend to drive the system into a metallic state.[4] For the present case of a surface with half-integer doping, the nearest-neighbor Coulomb repulsion V becomes important in defining the transport properties, since U no longer constitutes a barrier for transfer of an electron from doubly to singly charged sites, allowing metallic conduction in principle. To see this explicitly, we note that the differently charged fullerenes can in principle arrange themselves as a charge-density wave (CDW) as illustrated in Fig. 6.

This configuration corresponds to an insulating state with a gap of $2V$. To see this, it is necessary to consider the total energy in a given electron transfer process. We begin with the transfer of an electron from a molecule at −2 to a site with charge −1, but not a nearest-neighbor, i.e., far enough away to ignore interactions between the initial and final molecules. Underlying this approach is the assumption that, because the one-electron LUMO-derived band is quite narrow,[10] we can ignore the slight difference in binding energy due to that aspect of the local charge state, and focus on the differences in the correlation contributions. For the initial state of the starting molecule, these amount to Coulomb energies proportional to the local charge times the nearest-neighbor charges times V, or $E^I_{-2}=2(2\cdot 2+4\cdot 1)V=16V$. The initial state correlation contribution of the target molecule in the transfer is similarly derived to be $E^I_{-1}=1(4\cdot 2+2\cdot 1)V=10V$. The local correlation-dependent energy of the starting configuration is then $E^I=E^I_{-2}+E^I_{-1}=26V$. After the transfer, we carry out similar calculations for the two sites, obtaining $E^F=28V$. Thus the energy input to the system required for this transition is $\Delta E=E^F-E^I=2V$, which is the minimum energy for complete separation of the transported charge from its original site, and corresponds to the fundamental gap of a correlated insulator. Transfer to a nearest-neighbor singly charged site, on the other hand, costs only V (note the need to avoid double-counting the mutual interaction), and corresponds to a charge transfer exciton for the surface layer. As we show below the CDW is not the only solution for the ground state of the half-integer-charged surface layer, but serves as a starting point for considering its properties, and we will now examine the consequences expected in PES.

Calculating the absolute binding energy in PES of this system is a task far beyond the scope of the present work. Instead, we focus on the difference in binding energy of the two surface sites, analogously to the electron transfer calculations above. PES corresponds to electron removal, and so we calculate the correlation contributions to the binding energies.

We seek, therefore, electron removal energies from singly and doubly charged sites. We have shown above that the initial state term in the former case is $E^{I-PES}_{-1}=10V$. For the doubly charged site, we need to add the on-site contribution, U, which is the repulsion between the two conduction band electrons on the given molecule, to the previous calculation, giving $E^{I-PES}_{-2}=U+16V$.

The final state energies are calculated similarly. $E^{F-PES}_{-1}=0$ and $E^{F-PES}_{-2}=8V$. These yield net changes of $\Delta E^{PES}_{-1}=E^{F-PES}_{-1}-E^{I-PES}_{-1}=10V$ and $\Delta E^{PES}_{-2}=E^{F-PES}_{-2}-E^{I-PES}_{-2}=U+8V$. The difference between these is then the predicted binding energy difference for PES from surface sites with the indicated net charge states, i.e., $\Delta E^{PES}_{Net}=U-2V$. Taking values of $U(\approx 1.1$ eV) and $V(\approx 0.35$ eV) for negatively charged molecules,[43] we obtain $\Delta E^{PES}_{Net}\approx 0.4$ eV. This splitting is illustrated as the separation between the surface sub-peaks, S1 and S2, of the C 1*s* given in Fig. 2(b), that is, it has the correct magnitude to rationalize the width of the C 1*s* surface component peak, which we take as support for the derivation given above.

Unique to a quantitative understanding of the LUMO-derived band is the fact that the number of electrons occupying this band varies as a function of molecular charge state, giving population-derived intensity factors of 1:2:3 (surface:surface:bulk), based on the discussion in Sec. III D. Because all other bands are fully occupied, the intensity factor for each of their spectral components is only a function of position in the sample (attenuation due to scattering), rather than local population. This already suggests the answer to the riddle of the fundamentally different line profiles for LUMO compared to all other bands, if the bulk molecular state is −3, since this factor compensates for the strong attenuation expected for the bulk portion of the spectrum, and the −1 and −2 charged molecules represent each only one-half monolayer, reducing their relative intensity by an extra factor of 2.[69] To model the spectra, however, some understanding of the expected line profiles and energetics is needed.

For the line profile of the bulk component of the LUMO, we simulate the vibrational structure using the gas phase spectrum[57] of C_{60}^{-}, which was broadened to mimic instrumental resolution and convoluted with a plasmon loss function[19,47] in line with previous work.[13] This approach worked well as a first approximation in a recent K_3C_{60} monolayer study.[22]

The line profile of each surface component is the next issue. The analysis above and depicted in Fig. 2(b) indicates that these, S1 and S2, are contained in the broad surface line shape, which is almost symmetric if the assumed scattering tail is excluded. Since both components are equal in intensity and derived from an insulator, we expect similar line shapes. As derived above, we take the splitting of the two surface charge states to be 0.4 eV. Thus the surface component should be split into two equal subcomponents, S1 and S2, shifted by this amount, as illustrated in Fig. 2(b). The same is then expected for the LUMO, with the intensity modification determined by population; the binding energy is given by the separation observed in the C 1*s*, placing the −2 contribution at about $E_F-0.6$ eV. The surface components are therefore represented by symmetric curves similar to the components in Fig. 2(c), scaled according to the assumed charge state.

The ratio between surface and bulk structure is taken from the analysis of the C 1*s* line shape.[58] The solid lines in Figs. 7(a) and 7(b) are the sums of these three components, taking electron multiplicity and surface-to-bulk ratio into account. It is apparent that this model gives semiquantitative agreement with the measured spectra, and it serves to explain their angle dependence.

Our model does not attempt to explain all details of the photoemission line shape; it is aimed at the angle dependence, with an assumption of common bulk and surface line shapes at both angles. It can be speculated, e.g., that coupling to intramolecular vibrations, origin of the structure appearing at about 0.25 eV, could be different from the gas phase results. Correlation satellites as well as effects due to incomplete charge transfer could be responsible for intensity at energies greater than 1 eV. These and similar details remain to be worked out. Thus we have succeeded to unify the picture of the *distribution of bulk and surface spectra* for the C 1*s*, LUMO-derived, and deeper valence bands.

Reexamining the PES of a single layer C_{60} doped to charge state −3 reported by Yang *et al.*[22] in terms of the present picture adds further insight. In Fig. 8 we compare the LUMO-derived band from that sample to our spectrum. Clearly, in the region where the surface states of solid K_3C_{60} appear in our model, less intensity is observed in the single layer spectrum, supporting our location of the charge states C_{60}^{-1} and C_{60}^{-2} in the solid K_3C_{60} spectrum.

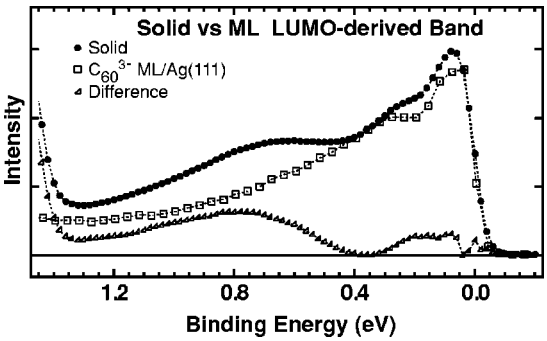

FIG. 8. Comparison of the present LUMO-derived photoemission spectrum to that of a K_3C_{60} monolayer (Ref. 22). The difference spectrum shows intensity at higher binding energy in the region of the expected surface contribution, as explained in the text.

It has been suggested elsewhere[25,35] that the surface layer of K_3C_{60} should be a metal due to the possibility of non-CDW charge configurations, which are equally stable. Spectroscopically, the large difference in binding energy, and especially the lack of significant intensity at E_F, suggests that this is not the case. Examining the metallic configurations, one finds that zero-cost transitions from −2 to −1 sites involve transfer over separations of at least two sites, which will presumably have a relatively low probability due to the small nearest-neighbor orbital overlap, suggesting that this is the reason that the surface exhibits primarily insulator character. The width of the individual surface lines consistent with the analysis above could be due in part to a distribution of local (non-CDW) charge configurations, leading to final states with energies above and below the main candidates already discussed, but otherwise conforming to the same general description.

F. K spectra

The bulk signal in the K-derived spectra (2*p* and 3*p*) is expected to show two components reflecting the tetrahedral and octahedral lattice sites occupied by the alkali atoms. K 2*p* spectra recorded with Al $K\alpha$ excitation show two components close to the theoretical intensity ratio[14,59] of 2:1. PES in the literature taken at different excitation energies, thus probing different sample depths, expose at least three components.[26] Spectra taken at lower excitation energy are shown in Fig. 9. The normal emission spectrum in Fig. 9(a) shows quite broad line shapes with several components. The components show a significant angle dependence, as shown in Fig. 9(b). This cannot be explained solely as being due to only two atomic sites. From our discussion of the surface structure it is clear that more than two bulklike components is reasonable: in principle, at least two octahedral and four tetrahedral surface components are also expected. To extract the contribution from the surface components we scale the

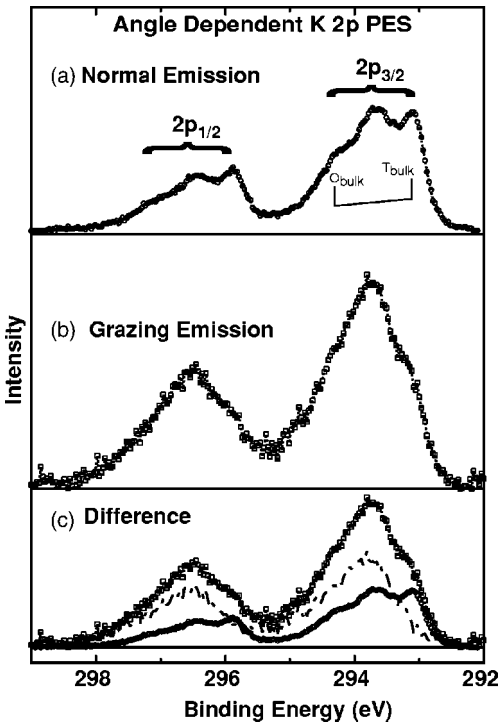

FIG. 9. (a), (b) K 2*p* photoemission of K_3C_{60} at the indicated emission angles, taken at $h\nu$=365 eV. The contributions of inelastically scattered photoelectrons were subtracted after estimation of a Shirley background. The separation of bulk tetrahedral and octahedral sites as previously determined in Ref. 59 is indicated. (c) The difference between normal and grazing emission shown as a dashed line was determined using the illustrated rescaled spectra of (a) and (b). The difference should be a good approximation to the surface line shape. The analysis is not as straight forward as in the C 1*s* region, which is rationalized in the present model as due to the existence of several K surface sites.

normal emission data to match the grazing emission data at the shoulder as shown in Fig. 9(c). Since the surface shows contributions from different depths, however, it is not possible to isolate the bulk contribution using this procedure. This suggests that the bulk is strong at lower binding energies (the tetrahedral component), but the octahedral component suggested by high photon energy data[14,59] is difficult to isolate in the data. Further support for this assignment is given in Fig. 10, where we compare K 3*p* spectra acquired at different excitation energies. Once again, the low-binding-energy component is enhanced at high excitation energies, which supports the present model. The fact that more than two components are observed is an additional challenge to the consensus model of a bulklike surface, since the placement, if not the number as suggested here, of the K ions relative to the surface fulleride layer must differ substantially from that of the bulk. The broad shape of the surface emission is also supportive of the present model with several K sites expected to contribute.

IV. INFLUENCE OF THE LIGHT POLARIZATION

Recent studies on solid C_{60} have established that the photoelectron cross section is largely that of the free molecule,

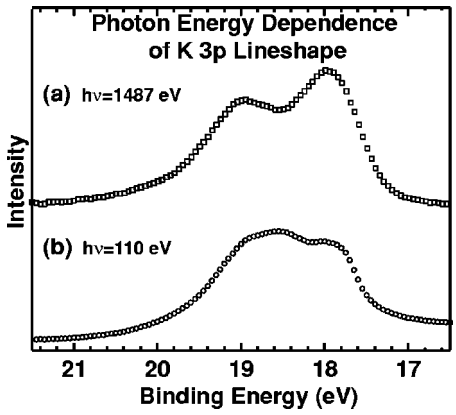

FIG. 10. K 3*p* PES at the indicated excitation energies.

which for nonoriented molecules places the strongest emission along the light polarization direction.[42] The same effect is observed for K_3C_{60}, making it paramount to exploit when measuring the band profiles. To illustrate this, we have measured spectra in different geometries, e.g., with polarization kept normal to the surface, and observed for these cases as well a decrease of the features at the low-binding-energy side of the C 1*s* and valence subband as well as the signal at E_F with respect to the rest of the LUMO-derived band. Our observation is that the electrons are emitted most strongly along the polarization direction, and if one holds that direction fixed (e.g., along the surface normal), then spectra taken at other angles will obtain relatively strong contributions from the electrons which were scattered out of the primary emission cone. Photoemission of the LUMO-derived band is shown for both cases in Fig. 11. The light polarization is fixed in Fig. 11(a) and is always along the emission direction in Fig. 11(b). Keeping the light polarization along the measured electron emission direction minimizes the effects of inelastically scattered photoelectrons, so that the high-energy tail changes relatively little for grazing emission. This observation is one possible explanation for the range of values reported for the "mean free path" in such samples. It also rationalizes the lack of angle dependence previously reported

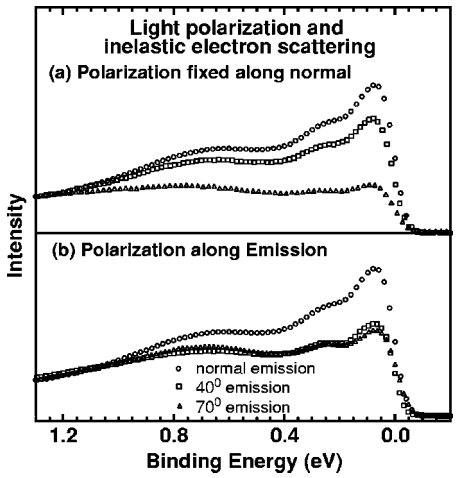

FIG. 11. Angle-dependent PES spectra of the K_3C_{60} LUMO-derived band at the indicated angles and polarization settings.

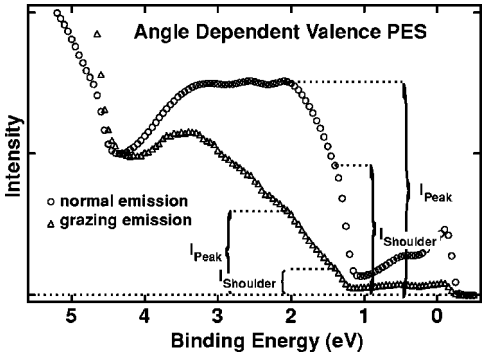

FIG. 12. Valence PES of K_3C_{60} taken at 110 eV at the indicated emission angles. The light polarization direction was parallel to the electron emission direction. The height of peaks and shoulders is indicated by braces. The ratio of peak height to shoulder intensity is 1.6 in normal emission and 3.4 in grazing emission.

for K_3C_{60} using unpolarized light,[13,16] due to the fact that the strongest emission was never in the measurement direction, and so strong contributions from scattered electrons would be expected in all measurement angles. Since we have found that the polarization direction determines the primary emission cone of the electrons for fullerene solids, the choice we have presented here is the optimal one for comparing mean free path effects on the emission intensities.

A valence spectrum taken in the condition of light polarization along the emission direction is shown in Fig. 12. The ratio between HOMO peak and shoulder increases for grazing emission. It is important to note that we observe a similar angle dependence in all spectra, C 1*s*, HOMO-derived, and the LUMO-derived bands. Thus from our studies, we can state that, regardless of the polarization direction chosen, the C 1*s* and valence spectra show the same qualitative trends as a function of electron emission angle. This is what one expects if the low-binding-energy features are due to subsurface species, and the higher-binding energy features to surface species.

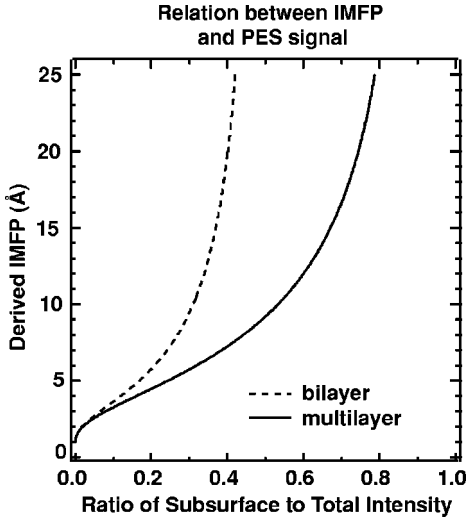

FIG. 13. The IMFP of photoelectrons for the indicated samples. See the text for more details.

V. DISCUSSION

We have shown thus far that the consensus picture of the surface composition and electronic structure of K_3C_{60} being similar to the bulk is not justified, using the following observations: (1) The splitting of the C 1*s* level requires at least two different molecular charge states, one in the surface and one in the bulk; (2) Uniform binding energy shifts among all levels for charge transfer compounds require a common explanation for the LUMO, HOMO, and C 1*s* bands; in combination with the most likely surface structure, this suggests two surface valences (−1 and −2), and one bulk valence (−3), which gives a semiquantitative explanation of the observed width in the surface component, and the observed LUMO line shape; (3) The widths of the bulk and surface K_3C_{60} spectra are now understood to be much smaller, in line with monolayer observations and with theory; and (4) The doping dependence of the spectra, in particular the E_F-to-HOMO-shoulder correlation, is well-understood in terms of changing molecular charge states, since those portions of the spectra belong to −3-charged molecules. This also rules out the existence of a surface superconductor, since the gap-opening at E_F observed in PES experiments[37] must be attributed to the bulk, and is therefore consistent with expectations based on transport measurements.[1] There are, however, two remaining issues to consider.

A. Temperature effects

There is a common temperature dependence of the bulk HOMO component and the intensity at E_F.[19] Note that the small feature between HOMO and HOMO-1, and the small shoulder on the low-binding energy side of HOMO-2 (see Fig. 1 of Ref. 19) vanish at higher temperature in the same manner, which is an expected correspondence in our model. The C 1*s* line exhibits similar changes as the temperature is increased.[26] We propose that this can be explained as an effect of disorder at increasing temperature decreasing the intensity of the bulk relative to the surface component. These effects have in principle several possible explanations, most of which can be ruled out. Coupling to intramolecular vibrations is well-known to generally increase the level of broadening with increased temperature, but for fullerenes has no other major effect (see, e.g., Refs. 60 and 61). A change in the charge density could cause major shifts of the core and deeper valence lines as the lattice expands, or upon redistribution of K within or even out of the sample, but this would not explain the observation at E_F of similar intensity decreases as for the HOMO and C 1*s* shoulders. In particular, the temperature effects are reversible, suggesting that K does not strongly redistribute itself; also, the sample remains largely metallic throughout most, if not all, of the observed temperature range, though there are speculations that there may be a metal-insulator transition in the higher range of temperatures studied.[62]

A recent study on an Al surface[63] shows similar variations in surface to bulk intensity at increasing temperature quite clearly, if one examines their Fig. 1. They show that the identifiable bulk intensity is strongly redistributed due to intrinsic phonon coupling, and can be decomposed according

to the number of phonons absorbed or emitted. This would explain how the intermolecular vibrations contribute to the broadening in the spectra, but could not explain intensity redistributions of the scale observed here, especially considering the low energy of those phonons.

We propose instead that the similarity in temperature-induced effects in C 1*s*, HOMO-derived, and LUMO-derived-bands can be understood in terms of a decreased effective IMFP at higher temperatures. Due to the higher probability for elastic and near-elastic scattering at elevated temperatures, electrons originating from deeper layers will travel a longer path before reaching the surface, thereby increasing their chance of inelastic scattering relative to that of electrons emitted from the surface layer. Hence the effective IMFP decreases at higher temperatures. This would explain the reduced bulk signal in the spectrum. In our case, with a weak bulk signal to begin with, the surface signal will increasingly dominate as the temperature increases. This simple explanation appears to be the only one consistent with the temperature-dependent observations, and is also supportive of the present model.[64]

B. EELS

Using EELS Goldoni *et al.* conclude that the surface and bulk electronic structure of K_3C_{60} are quite similar.[18] Since the surface layer has charge states −1 and −2 in our model, a reduced plasmon loss, presumably at a much lower energy, would be expected. Studies of mixed phases do not show any signal in the energy range up to 0.6 eV from lower stoichiometries in EELS.[65] In this picture the observed plasmon loss for K_3C_{60} would then be assigned to the first and deeper bulk layers at low temperature. As the temperature is increased, electron-vibration scattering increases, thus causing the surface signal to increasingly dominate, assuming the mechanism proposed in Sec. V A applies. Considering the largely insulating character at lower charge state deduced for this layer, it is not clear which excitations should arise, but, e.g., plasmon excitation would be presumably lower in energy, perhaps dwarfed by the elastic beam. We can also assume that at elevated temperatures the Fermi-Dirac distribution will reduce the number of occupied states below E_F, perhaps thereby reducing the plasmon energy itself, rationalizing the EELS observation of a slight energy decrease at higher temperature.[66] Thus the EELS results of Ref. 18 appear to be reasonably reconciled with our interpretation of the photoelectron spectra in a simple manner.

VI. CONCLUSIONS

We have reported an angle dependence in the C 1*s*, HOMO- and LUMO-derived bands of K_3C_{60}, pointing towards an insulating surface and metallic bulk. We have summarized work in literature and found a constant separation in energy between C 1*s* and HOMO-derived bands in all charge transfer C_{60} systems. Based on the constant separation and on our observations we developed a model that identifies common features in core level and valence spectra.

This model enabled us to resolve major difficulties in previous interpretations of similar data. It explains the broad photoemission line shapes in terms of bulk and surface electronic structure consistently in the K 2*p*, C 1*s*, and valence spectra. Our analysis shows that the LUMO-derived band can be modeled as a bulk line at the Fermi level which resembles gas phase data in its vibronic structure, consistent with previous work,[13,16,22] plus two surface lines at higher binding energy, and with intensities scaled by mean free path and population effects. Thus our result suggests that the correlated surface of K_3C_{60} is an insulator, or at best, a poor metal, a situation driven by the dominance of the intermolecular electron-electron correlations at the surface.

Note added in proof. Recently, we discovered an EELS study (Ref. 73) which comes to similar conclusions about the surface electronic structure based on vibrational energies. Also, some additional details relevant to the present work may be found in Ref. 74.

ACKNOWLEDGMENTS

We would like to thank W. Eberhardt and W. L. Yang for making the C_{60}^- and the doped C_{60} monolayer data, respectively, available to us, and O. Gunnarsson, G. A. Sawatzky, L. H. Tjeng, A. Goldoni, and J. Fink for stimulating discussions. This work was performed within the EU-TMR "FULPROP" network, Contract No. ERBFMRX-CT97-0155, with additional funding from the EU Access to Large Scale Facilities Program. I. Marenne acknowledges the FRIA, Belgium, for financial support. J. Schiessling acknowledges financial support during the writing of parts of the manuscript by the University of Groningen. We would also like to acknowledge the Belgian National Fund for Scientific Research (FNRS), FOM (Netherlands), the Consortium on Clusters and Ultrafine Particles and the Caramel Consortium for financial support, which in turn were supported by Stiftelsen för Strategisk Forskning, as well as, Vetenskapsrådet and Göran Gustafsons Stiftelse.

APPENDIX: ADDITIONAL ASPECTS OF THE IMFP IN C_{60} SOLIDS

If we reexamine the published IMFP values in terms of the intensities which they imply, we find that all published results are consistent within the experimental uncertainties. Wertheim *et al.*[11] report 6 Å, Goldoni *et al.*[18] 4.7^{+2}_{-1} Å, which gives contributions from the bulk signal of 32% and 22^{+12}_{-10}%, respectively. In the study by Wertheim *et al.* no error bars were declared; however, these can be assumed to be of the same order of magnitude as in the other study. Maxwell *et al.* show a contribution from the bottom layer in a two layer system of 38^{+7}_{-10}%. To better understand these results, we calculate the expected intensity for a given IMFP.

As a first approximation, the photoemission intensity of a system consisting of a surface layer and *m* subsurface layers is calculated via a sum of exponential functions with a primary intensity I_0:

$$I_{\mathrm{surf}} = I_0 e^{-5\ \text{Å}/\lambda};$$

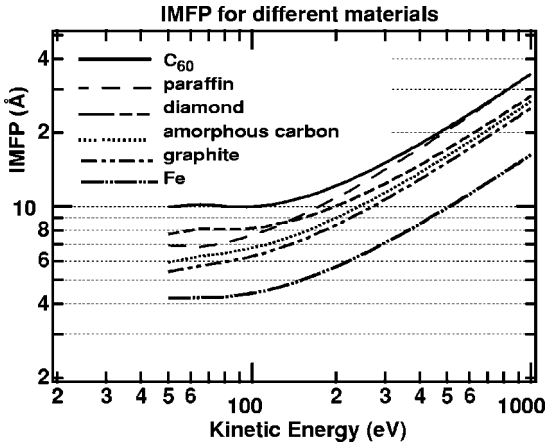

FIG. 14. Calculated IMFPs from the TPP-2M formulas for the set of materials as shown in Table II as a function of kinetic energy.

$$I_{\text{subsurf}} = \Sigma_{n=1}^{m} I_0 e^{-(5+8n)\ \text{Å}/\lambda}, \tag{A1}$$

where the length of the path the photoelectron originating from the *n*th subsurface layer has to travel to the surface is given by the numerator in the exponent, $(5+8n)$ Å. The IMFP is denoted by λ. The size of the C_{60} molecule is 10 Å.[70] We therefore assume that the photoemission signal originates on average 5 Å below the top of a given layer. The layer separation is taken to be 8 Å, equal to the spacing in a crystal. The relative contribution of the subsurface layers is given by the ratio

$$R_{\text{subsurf},m} = I_{\text{subsurf},m}/(I_{\text{subsurf},m} + I_{\text{surf}}), \tag{A2}$$

where $m=2$ ($m=\infty$) for a bilayer (semi-infinite) system. As shown in Fig. 13, the IMFP as estimated using PES intensities diverges for larger subsurface contributions, emphasizing the importance of monitoring the uncertainties in the measured intensities. For example, for a ratio of 38^{+7}_{-10}% as obtained from the bilayer system studied by Maxwell *et al.*[28] the IMFP is properly given by 16.3^{+25}_{-8} Å. Thus within the given error bars the contribution from bulk molecules in C_{60} solids can be expected to be in the range of 20%–30% of the total photoemission signal for $h\nu=110$ eV.

Now we compare this result with the general case. An IMFP of the order of 16 Å at the photon energy of 100 eV is somewhat larger than expected from the "universal curve" for elements. To a first approximation the IMFP is a function of kinetic energy, whose shape is almost independent of the material.[24] This can be understood from the argument that the cross section for inelastic electron scattering depends on the valence electron density, which is almost a constant for metals, explaining the general behavior for those systems. Calculations of the universal curve carried out by Tanuma *et al.*[40] give good agreement with experimental data. A more detailed study of organic compounds, however, gives values of the IMFP larger than expected from the universal curve for metals.[41] This deviation has its origin in the lower density and different plasmon energies for these systems.

The IMFP λ in solid elements and compounds at electron energies of more than 50 eV can be obtained with good accuracy with the TPP-2M equation of Tanuma *et al.*:[41,72]

$$\lambda = E/\{E_p^2[\beta \ln(\gamma E) - (C/E) + (D/E^2)]\}, \tag{A3}$$

$$\beta = -0.10 + 0.944/\sqrt{E_P^2 + E_g^2} + 0.069\rho^{0.1}, \tag{A4}$$

$$\gamma = 0.191\rho^{-0.5}, \tag{A5}$$

$$C = 1.97 - 0.91E_P^2/829.4, \tag{A6}$$

$$D = 53.4 - 20.8E_P^2/829.4, \tag{A7}$$

with E_P as the free-electron plasmon energy,

$$E_P = 28.8\sqrt{\frac{N_V\rho}{M}} \tag{A8}$$

ρ is the density, N_V the number of valence electrons per atom/molecule, M the atomic/molecular weight, and E_g the energy gap.

In Fig. 14 the IMFP is calculated from Eq. (A3) for different metallic and organic systems; the parameters used are summarized in Table II. The curves for the metals display the lowest IMFP, whereas the IMFP for organic compounds can be up to a factor of 2 larger. Thus for the interpretation of photoemission results of organic compounds the universal curve for elements gives values which are too small. C_{60}, in particular, is expected to show a relatively high IMFP, in contrast to earlier assumptions.[11]

TABLE II. Parameters used for the TPP-2M equation. Values of the parameters β, γ, C, and D were calculated, except for paraffin and iron, where the parameters were taken from fits of Eq. (A3) to experimental IMFP data. For cases in which E_P was calculated from the given values for N_V, ρ, and M, the resulting value is set in parenthesis.

Compound	β (eV^{-1} Å^{-1})	γ (eV^{-1})	C (Å^{-1})	D (eV Å^{-1})	ρ (g cm^{-3})	M	N_V	E_p (eV)	E_g (eV)
C (amorph)	0.0141	0.135	1.36	39.5	2	12	4	(23.5)	1.6
graphite	0.0157	0.129	1.390	40.1	2.2			23 (Ref. 66)	0
diamond	0.0080	0.102	0.902	29.0	3.51	12	4	(31.17)	5.4
C_{60}	0.0085	0.146	1.205	35.9	1.72 (Ref. 66)			26.4 (Ref. 66)	1.6
26-n-Paraffin	0.0160	0.175	1.01	14.9				18.8	6
Fe	0.0155	0.0742	0.991	30.5				30.6	

*Electronic address: joachim.schiessling@fysik.uu.se
†Present address: MAX-lab, University of Lund, Box 118, SE-221 00 Lund, Sweden.
‡Present address: Institute of Physics, Tartu University, Riia 142, EE-51014 Tartu, Estonia.
§Present address: School of Physics and Astronomy, University of Nottingham, Nottingham, NG7 2RD, United Kingdom.
‖Present address: Department of Physics and Astronomy, University of Aarhus, Ny Munkegade, 8000 Aarhus C, Denmark.
¶Present address: Department of Electronic Materials Engineering, Research School of Physical Sciences and Engineering, Australian National University Canberra, Australia.
**Present address: Process Chemical Physics, Department of Materials Science and Engineering, Kyoto University, Skyo-ku, Kyoto 606-8501, Japan.
††Present address: Institut de physique, Université de Neuchâtel rue Breguet 1, CH-2000 Neuchâtel, Switzerland.
‡‡Electronic address: paul.bruehwiler@empa.ch

[1] O. Gunnarsson, Rev. Mod. Phys. **69**, 575 (1997).
[2] M. Fabrizio and E. Tosatti, Phys. Rev. B **55**, 13 465 (1997).
[3] M. Knupfer and J. Fink, Phys. Rev. Lett. **79**, 2714 (1997).
[4] J. E. Han, E. Koch, and O. Gunnarsson, Phys. Rev. Lett. **84**, 1276 (2000).
[5] J. E. Han, O. Gunnarsson, and V. H. Crespi, Phys. Rev. Lett. **90**, 167006 (2003).
[6] Y. Iwasa and T. Takenobu, J. Phys.: Condens. Matter **15**, R495 (2003).
[7] P. J. Benning, J. L. Martins, J. H. Weaver, L. P. F. Chibante, and R. E. Smalley, Science **252**, 1417 (1991).
[8] G. K. Wertheim, J. E. Rowe, D. N. E. Buchanan, E. E. Chaban, A. F. Hebard, A. R. Kortan, A. V. Makhija, and R. C. Haddon, Science **252**, 1419 (1991).
[9] C. T. Chen, L. H. Tjeng, P. Rudolf, G. Meigs, J. E. Rowe, J. Chen, J. P. McCauley, A. B. Smith, A. R. McGhie, W. J. Romanow, and E. W. Plummer, Nature (London) **352**, 603 (1991).
[10] S. Satpathy, V. P. Antropov, O. K. Andersen, O. Jepsen, O. Gunnarsson, and A. I. Liechtenstein, Phys. Rev. B **46**, 1773 (1992).
[11] G. K. Wertheim, D. N. E. Buchanan, E. E. Chaban, and J. E. Rowe, Solid State Commun. **83**, 785 (1992).
[12] G. K. Wertheim and D. N. E. Buchanan, Phys. Rev. B **47**, 12 912 (1993).
[13] M. Knupfer, M. Merkel, M. S. Golden, J. Fink, O. Gunnarsson, and V. P. Antropov, Phys. Rev. B **47**, 13 944 (1993).
[14] P. A. Brühwiler, A. J. Maxwell, A. Nilsson, N. Mårtensson, and O. Gunnarsson, Phys. Rev. B **48**, 18 296 (1993).
[15] D. M. Poirier, Appl. Phys. Lett. **64**, 1356 (1994).
[16] A. Goldoni, S. L. Friedmann, Z.-X. Shen, and F. Parmigiani, Phys. Rev. B **58**, 11 023 (1998).
[17] P. J. Benning, F. Stepniak, D. M. Poirier, J. L. Martins, J. H. Weaver, L. P. F. Chibante, and R. E. Smalley, Phys. Rev. B **47**, 13 843 (1993).
[18] A. Goldoni, L. Sangaletti, F. Parmigiani, G. Comelli, and G. Paolucci, Phys. Rev. Lett. **87**, 076401 (2001).
[19] A. Goldoni, L. Sangaletti, S. L. Friedmann, Z.-X. Shen, M. Peloi, F. Parmigiani, G. Comelli, and G. Paolucci, J. Chem. Phys. **113**, 8266 (2000).
[20] R. W. Lof, M. A. van Veenendaal, B. Koopmans, H. T. Jonkman, and G. A. Sawatzky, Phys. Rev. Lett. **68**, 3924 (1992).
[21] L. H. Tjeng, R. Hesper, A. C. L. Heessels, A. Heeres, H. T. Jonkmann, and G. A. Sawatzky, Solid State Commun. **103**, 31 (1997).
[22] W. L. Yang, V. Brouet, X. J. Zhou, H. J. Choi, S. G. Louie, M. L. Cohen, S. A. Kellar, P. V. Bogdanov, A. Lanzara, A. Goldoni, F. Parmigiani, Z. Hussain, and Z.-X. Shen, Science **300**, 303 (2003).
[23] R. Hesper, L. H. Tjeng, and G. A. Sawatzky, Europhys. Lett. **40**, 177 (1997).
[24] S. Hüfner, *Photoelectron Spectroscopy* (Springer-Verlag, Berlin, 1996).
[25] R. Hesper, Ph.D. thesis, Rijksuniversiteit Groningen, 2000.
[26] A. Goldoni, L. Sangaletti, F. Parmigiani, S. L. Friedmann, Z.-X. Shen, M. Peloi, G. Comelli, and G. Paolucci, Phys. Rev. B **59**, 16 071 (1999).
[27] W. Andreoni, P. Giannozzi, and M. Parrinello, Phys. Rev. B **51**, 2087 (1995).
[28] A. J. Maxwell, P. A. Brühwiler, A. Nilsson, N. Mårtensson, and P. Rudolf, Phys. Rev. B **49**, 10 717 (1994).
[29] E. Magnano, S. Vandré, C. Cepek, A. Goldoni, A. D. Laine, G. M. Curró, A. Santaniello, and M. Sancrotti, Surf. Sci. **377–379**, 1066 (1997).
[30] K.-D. Tsuei, J.-Y. Yuh, C.-T. Tzeng, R.-Y. Chu, S.-C. Chung, and K.-L. Tsang, Phys. Rev. B **56**, 15 412 (1997).
[31] A. J. Maxwell, P. A. Brühwiler, D. Arvanitis, J. Hasselström, M. K.-J. Johansson, and N. Mårtensson, Phys. Rev. B **57**, 7312 (1998).
[32] M. Pedio, K. Hevesi, N. Zema, M. Capozi, P. Perfetti, R. Gouttebaron, J.-J. Pireaux, R. Caudano, and P. Rudolf, Surf. Sci. **437**, 249 (1999).
[33] E. Rotenberg, C. Enkvist, P. A. Brühwiler, A. J. Maxwell, and N. Mårtensson, Phys. Rev. B **54**, R5279 (1996).
[34] J. van den Brink and G. A. Sawatzky, Europhys. Lett. **50**, 447 (2000).
[35] R. Hesper, L. H. Tjeng, A. Heeres, and G. A. Sawatzky, Phys. Rev. B **62**, 16 046 (2000).
[36] Y. B. Zhao, D. M. Poirier, and J. H. Weaver, J. Phys. Chem. Solids **54**, 1685 (1993).
[37] R. Hesper, L. H. Tjeng, A. Heeres, and G. A. Sawatzky, Phys. Rev. Lett. **85**, 1970 (2000).
[38] J. H. Weaver, J. L. Martins, T. Komeda, Y. Chen, T. R. Ohno, G. H. Kroll, N. Troullier, R. E. Haufler, and R. E. Smalley, Phys. Rev. Lett. **66**, 1741 (1991).
[39] A. Jablonski and C. J. Powell, J. Electron Spectrosc. Relat. Phenom. **100**, 137 (1999).
[40] S. Tanuma, C. J. Powell, and D. R. Penn, Surf. Interface Anal. **11**, 577 (1988).
[41] S. Tanuma, C. J. Powell, and D. R. Penn, Surf. Interface Anal. **21**, 165 (1993).
[42] J. Schiessling, L. Kjeldgaard, T. Balasubramanian, J. Nordgren, and P. A. Brühwiler, Phys. Rev. B **68**, 205405 (2003).
[43] V. P. Antropov, O. Gunnarsson, and O. Jepsen, Phys. Rev. B **46**, R13 647 (1992).
[44] R. Denecke, P. Väterlein, M. Bässler, N. Wassdahl, S. M. Butorin, A. Nilsson, J.-E. Rubensson, J. Nordgren, N. Mårtensson, and R. Nyholm, J. Electron Spectrosc. Relat. Phenom. **103**, 971 (1999).
[45] D. Nordlund, M. G. Garnier, N. Witkowski, R. Denecke, A. Nilsson, M. Nagasono, N. Mårtensson, and A. Föhlisch, Phys. Rev. B **63**, 121402(R) (2000).
[46] R. Fasel, R. G. Agostino, P. Aebi, and L. Schlapbach, Phys. Rev. B **60**, 4517 (1999).
[47] A. I. Liechtenstein, O. Gunnarsson, M. Knupfer, J. Fink, and J. F.

Armbruster, J. Phys.: Condens. Matter **8**, 4001 (1996).
[48] A. J. Maxwell, P. A. Brühwiler, D. Arvantis, J. Hasselström, and N. Mårtensson, Chem. Phys. Lett. **260**, 71 (1996).
[49] C.-T. Tzeng, W.-S. Lo, J.-Y. Yuh, R.-Y. Chu, and K.-D. Tsuei, Phys. Rev. B **61**, 2263 (2000).
[50] C. Cepek, P. Schiavuta, M. Sancrotti, and M. Pedio, Phys. Rev. B **60**, 2068 (1999).
[51] Y. Chao, K. Svensson, D. Radosavkić, V. R. Dhanak, L. Śiller, and M. R. C. Hunt, Phys. Rev. B **64**, 235331 (2001).
[52] P. Bennich, C. Puglia, P. A. Brühwiler, A. Nilsson, A. J. Maxwell, A. Sandell, N. Mårtensson, and P. Rudolf, Phys. Rev. B **59**, 8292 (1999).
[53] M. Montalti, S. Krishnamurthy, Y. Chao, Y. V. Butenko, V. L. Kuznetsov, V. R. Dhanak, M. R. C. Hunt, and L. Siller, Phys. Rev. B **67**, 113401 (2003).
[54] K. Sakamoto, T. Wakita, D. Kondo, A. Harasawa, T. Kinoshita, W. Uchida, and A. Kasuya, Surf. Sci. **499**, 63 (2002).
[55] M. Merkel, M. Knupfer, M. S. Golden, J. Fink, R. Seemann, and R. L. Johnson, Phys. Rev. B **47**, 11470 (1993).
[56] S. C. Erwin and M. R. Pederson, Phys. Rev. Lett. **67**, 1610 (1991).
[57] O. Gunnarsson, H. Handschuh, P. S. Bechthold, B. Kessler, G. Ganteför, and W. Eberhardt, Phys. Rev. Lett. **74**, 1875 (1995).
[58] In Fig. 4 we have demonstrated the coincidence between the C 1*s* and valence line shapes. In the spectra the photoelectrons have comparable kinetic energies. Since the C 1*s* line shape matches that of the HOMO-derived band, the surface and bulk contributions are comparable in both cases, and we can use this information to model the LUMO-derived PES data.
[59] D. M. Poirier, T. R. Ohno, G. H. Kroll, P. J. Benning, F. Stepniak, J. H. Weaver, L. P. F. Chibante, and R. E. Smalley, Phys. Rev. B **47**, 9870 (1993).
[60] T. Takayashi, T. Morimoto, A. Ito, and T. Yokoya, Solid State Commun. **92**, 331 (1994).
[61] N. Manini, P. Gattari, and E. Tosatti, Phys. Rev. Lett. **91**, 196402 (2003).
[62] V. Brouet, H. Alloul, S. Garaj, and L. Forro, Phys. Rev. B **66**, 155124 (2002).
[63] C. Søndergaard, P. Hofmann, C. Schultz, M. S. Moreno, J. E. Gayone, M. A. V. Alvarez, G. Zampieri, S. Lizzit, and A. Baraldi, Phys. Rev. B **63**, 233102 (2001).
[64] Of course, if a metal-insulator transition occurs (Ref. 61), we would only apply this model at lower temperatures, and would need to understand the changes in line shape expected in such a phase to make sensible conclusions of the consequences, though the presently proposed mechanism would remain active to a similar extent. Such a phase is at this point speculative, and a transition temperature has not been identified.
[65] M. F. Luo, Z. Y. Li, and W. Allison, Surf. Sci. **523**, 168 (2003).
[66] E. T. Jensen, R. E. Palmer, W. Allison, and J. F. Annett, Phys. Rev. Lett. **66**, 492 (1991).
[67] To good first approximation, assuming complete charge transfer from K to C_{60} (Ref. 56).
[68] Including the spectra from a third angle does not materially improve the line-shape determination, since the scattering effects at high binding energy also change with angle.
[69] This factor of 2 is not taken up explicitly in what follows, since it is automatically included in the experimental intensity measured here, and follows naturally for the C 1*s* and deeper valence spectra from the separation of the surface component into two subcomponents. It serves to explain, however, how the bulk states can easily be seen in the LUMO-derived spectrum.
[70] The diameter of the sphere formed by the carbon atoms of C_{60} is 7 Å. In addition the size of the π-electron cloud associated with the carbon atoms has to be taken into account, which gives the van der Waals diameter of approximately 10 Å (Ref. 71).
[71] M. S. Dresselhaus, G. Dresselhaus, and P. C. Eklund, *Science of Fullerenes and Carbon Nanotubes* (Academic Press, San Diego, 1996).
[72] http://www.nist.gov/srd/webguide/nist71/71imfp.htm
[73] C. Silien, P. A. Thirty, and Y. Caudano, Phys. Rev. B **67**, 075412 (2003).
[74] J. Schiessling, L. Kjeldgaard, T. Käämbre, I. Marenne, L. Qian, J. N. O'Shea, J. Schnadt, M. G. Garnier, D. Nordlund, M. Nagasono, C. J. Glover, J.-E Rubensson, N. Mårtensson, P. Rudolf, J. Nordgren, and P. A. Brühwiler, Eur. Phys. J. B **41**, 431 (2004).